Int. J. Heat Mass Transfer. Vol. 31, No. 11, pp. 2357–2364, 1988
Printed in Great Britain

0017–9310/88 $3.00+0.00

Performance of an air-filled, open thermosyphon tube with particular reference to wind augmentation

G. S. H. LOCK and J. D. KIRCHNER
Department of Mechanical Engineering, University of Alberta, Edmonton, Alberta, Canada T6G 2G8

(*Received* 16 *December* 1987 *and in final form* 28 *April* 1988)

Abstract—The paper reports an experimental study of an air-filled, open tube thermosyphon. Following a review of thermosyphon regimes, with particular attention being given to the unusual features associated with air, a series of experiments are described. These were designed to explore the effect of a superimposed forced flow generated by prevailing winds. The effect of the wind, and the tubular arrangement necessary to channel it, are then discussed from a heat transfer standpoint.

INTRODUCTION

AS A HEAT transfer device, the open thermosyphon tube has received much attention. It has a wide range of potential applications, included among which are: heating of bakers' ovens [1], cooling of gas turbine blades [2, 3], refrigeration of moist soil [4, 5] and formation of underwater ice [6, 7]. In a geotechnical or geophysical context, the open thermosyphon tube exhibits the unique feature of thermal rectification. When the tube wall temperature is higher than that of the ambient air above, thermal energy is transferred upwards by means of natural convection, whereas when the temperature field is reversed, the convection system is absent and heat transfer then occurs through the less effective process of conduction. As a result of this feature, the winter cooling effect of the tube on surrounding material is very much greater than the summer heating effect. It is this winter cooling effect which is of principal importance in this paper.

The first theoretical study of the open thermosyphon tube was undertaken by Lighthill [8] who used a Von Karman–Pohlhausen integral analysis to reveal two basic flow regimes: a boundary layer regime in which hotter fluid rises in a thin annular layer adjacent to the wall, while cooler fluid simultaneously descends in a relatively large, slow-moving core; and an impeded regime in which the annulus and core are of comparable width, thus implying less effective convective transport. As will be seen later, it is the latter regime which is of major concern in this paper.

Theoretical work on the open thermosyphon has been extended by Japiske and Winter [9] who compared their results to the earlier predictions of Leslie and Martin [10]. By and large, the theoretical predictions of these authors are in good agreement with experimental findings, notable among which are the data of Martin [11] who appears to have been the first to report the unusual behaviour of the system when it is filled with air.

Typically, the heat transfer rate in an air-filled thermosyphon tube will be too low for it to be effective in a geotechnical application, where the overall heat transfer coefficient would likely exceed 10 W m^{-2} K^{-1}. To offset this disadvantage, it is here suggested that the prevailing wind may be used to augment natural circulation, thereby raising the heat transfer rate to the point where the device would become a practical alternative to the liquid-filled devices currently in use. The basic configuration is illustrated in Fig. 1 which shows a cowling device fitted to an insert tube such that the collected wind superimposes a forced convection effect on the natural convection which occurs whenever the air temperature is less than the tube wall temperature. We know of no previously published study of this system, although an exploratory numerical study in the absence of wind has appeared [12]. The main purpose of the present experimental work is to study the effect of the wind and the insert tube on heat transfer performance.

THE EXPERIMENTS

The rig

The experiments were conducted in the Department of Mechanical Engineering FROST† tunnel. This is a closed-loop wind tunnel in which the air temperature may be lowered from ambient to about −20°C, while the wind speed may be varied in the range 10–60 m s^{-1}. This air temperature range is less than may occur in a field situation but since the tube wall temperature in the laboratory may be raised well above the anticipated field value, the range of the overall temperature difference was not limited in practical terms. The lower level of wind speed, however, did pose a difficulty because the experiments were intended to cover

† An acronym for fundamental research on solidification and thawing.

NOMENCLATURE

a, b, c	coefficients
d	insert tube diameter
D	thermosyphon tube inner diameter
g	gravitational acceleration
Gz	Graetz number
h	heat transfer coefficient
k	thermal conductivity
L	tube length
m, n	exponents
Nu	Nusselt number
Pr	Prandtl number
P	static pressure
$\dot{Q}$	heat flux
Ra	Rayleigh number
Re	Reynolds number
T	absolute temperature
t	$Ra\,D/L$
U	air velocity.

Greek symbols

β	thermal expansion coefficient
ν	momentum diffusivity
κ	thermal diffusivity.

Subscripts

a	air (room)
D	thermosyphon tube diameter
i	insert tube
l	leakage
o	outside
w	wall
∞	wind.

Superscript

$\bar{}$	average.

a realistic range of *average* wind speeds, estimated to be between 0 and 20 m s^{-1}. The difficulty was overcome by sectioning of the tunnel with the device shown in Fig. 2. To create a quiescent environment of cold air, the device was positioned as shown in Fig. 2(a). The wire mesh on the trailing face acted as a filter and permitted a very slow circulation of air under the cover, thereby enabling the warm thermosyphon discharge to be continually mixed and removed. Figure 2(b) shows how the cover, with the mesh removed, was reversed to create a reduced wind speed by perforating the inclined portion, which originally faced upstream.

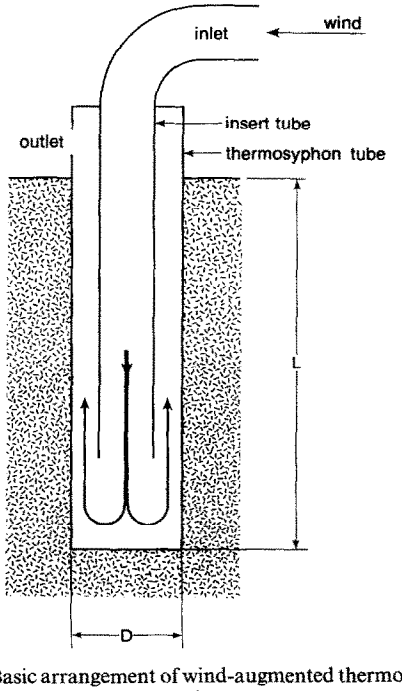

FIG. 1. Basic arrangement of wind-augmented thermosyphon tube.

The thermosyphons

The thermosyphons were constructed from copper tubes of various lengths, each with an inside diameter of 19.6 mm and an outside diameter of 22.2 mm. The insert tubes had inside and outside diameters of 12.7 and 15.9 mm, respectively. In choosing the dimensions of the insert tubes it was decided to treat the length as a variable in the experiments, but to fix the diameter so as to provide an approximation to equal flow areas for the ascending and descending air streams. The available core and annulus areas were 1.27 and 1.02 cm^2, respectively. The insert tube was made from polycarbonate material, which has a thermal conductivity of 2.3 W m^{-1} K^{-1}. Although not as good

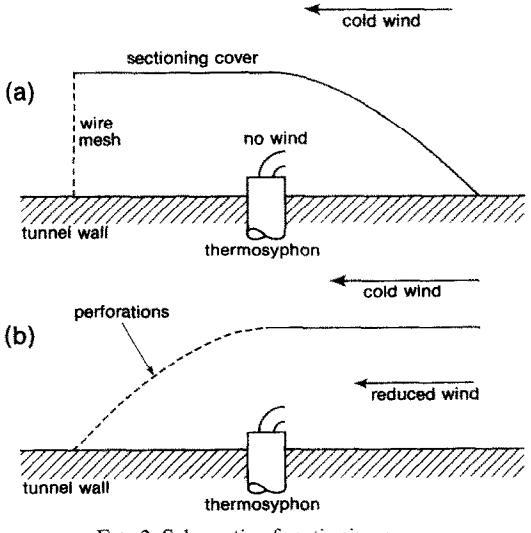

FIG. 2. Schematic of sectioning cover.

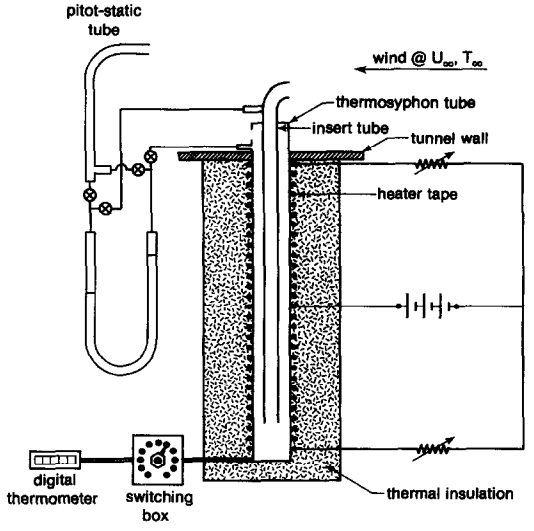

FIG. 3. Schematic of thermosyphon apparatus.

an insulator as air itself, the material is much better than a metal and helped control the heat leakage between the two air streams, thereby maintaining the core air near the wind temperature. Heat leakage from the outside of the thermosyphon was minimized with a wrapping of thermal insulation.

Several cowling designs were considered for the top of the thermosyphon, each being based on the idea that the dynamic head of the wind would provide the pressure difference driving the air through the tube. As a compromise between efficiency and simplicity, the design shown schematically in Fig. 1 was chosen. Air enters through a simple bend fitting and exits through two holes on the *sides* of the 'above-ground' thermosyphon extension at positions where the local static pressure would be at, or near, a minimum. Inlet and exit holes were located beyond the wall boundary layer of the tunnel. A schematic of the entire tube apparatus is shown in Fig. 3.

Instrumentation and calibration

As indicated, the tube was heated electrically using resistive metal tape wrapped around the tube wall after it had been insulated with a layer of fibreglass tape. Separate windings were used over two 10 cm lengths of tube thus providing some flexibility in approximating an isothermal tube wall;† temperature variations along the wall were typically less than $\pm 2°C$. Power was supplied to the heater tape by means of a Harrison 6286A d.c. unit (Hewlett Packard). The main controller and the variable resistors shown enabled the power levels to be adjusted in the range 0–50 W, as measured with ammeters and a voltmeter.

Temperatures were measured throughout by means of thermocouples located at 5 cm axial intervals (starting at 2.5 cm from the end) on the outside of the thermosyphon tube wall; they were also located in the wind (tunnel air) as well as in the ambient (room) air. The thermocouple signals were channelled through a switching box and read on a Fluke 2175A digital thermometer.

Wind speed nearby the cowling was measured with a pitot-static tube connected to a Dwyer Instruments microtector micromanometer, which was also used to measure the pressure drop within the thermosyphon tube, as indicated in Fig. 3. No attempt was made during the main tests to interrupt and monitor the air flow through the thermosyphon directly. Instead it was measured later, for the same pressure drop, by connecting the tube to an air supply connected in series with a rotameter: this reproduced internal flow conditions but not the inlet condition which was, however, believed to be a minor part of the overall pressure drop.

Prior to undertaking the experiments proper, the system was thermally calibrated so that the heat leakage could be calculated for any given condition and then subtracted from the power supply to the heater tape. The calibration consisted of plotting the power supply to the heater against the temperature difference between the tube wall and the ambient air when the tube was filled with granulated insulating material. This produced a relationship of the form

$$\dot{Q}_e = b(T_w - T_a) + f(U_\infty, T_\infty)$$

in which the first term on the right-hand side represents the linear conductive loss, essentially radial, through the surrounding insulation; the second term includes the convective losses into the cold FROST tunnel air. The latter is by far the smaller and may be represented by the forced convection relation $f = cU_\infty^m(T_w - T_\infty)$. The calibration curves thus served to provide the empirical constants b, c and m.

Experimental procedure

The experiments were conducted in the following manner. With a given length insert tube selected and installed, the FROST tunnel was started up and the wind speed and temperature set at pre-determined values: this usually required a period of 1–2 h before steady conditions were reached. In the meantime, the heater power was switched on and the level set to some particular, though arbitrary, value in the anticipated range. Over a period of about 3 h, adjustments were made in the individual heater supply rates in order to minimize longitudinal variations in tube wall temperature.

Once the system had attained steady, and acceptably uniform, conditions, readings of gross power, wind speed and temperature, tube pressure drop, tube wall temperature (at four locations), and ambient temperature were taken. These data, together with the calibration data, were then used to calculate the tube Nusselt number

† Strictly, this is a stepped heat flux condition but was satisfactory for present purposes, given the copper tube.

$$Nu_D = \frac{\bar{h}D}{k_a}$$

in which

$$\bar{h} = \frac{\dot{Q}_{net}}{\pi DL(T_w - T_\infty)}$$

the Rayleigh number

$$Ra_D = \frac{\beta g(T_w - T_\infty)D^3}{\nu\kappa}$$

and the tube Reynolds number $Re = \bar{U}\bar{D}/\nu$, in which $\bar{U}$ is the average velocity in the tube annulus, and $\bar{D} = D - d \simeq D/\sqrt{2}(\sqrt{2}+1)$.

Test schedule

The design of the experimental schedule was largely influenced by the behaviour of the system at zero wind speed, under which conditions the Nusselt number depends principally on the 'driving' term t_d defined by

$$t_d = Ra_D\frac{D}{L} = \frac{\beta g(T_w - T_a)D^4}{\nu\kappa L}.$$

To build a full-scale rig which used tube diameters and lengths representative of those expected in the field would have been prohibitively expensive. Fortunately, the concept of similitude reduces the need to do so, and thus allowed the use of an inexpensive copper tube 2 cm in nominal diameter and 20 cm long. This fixed the length–diameter ratio at 10:1.

Given the overall geometry of the system, it is clear that the smaller the tube diameter, the lower t_d will be and hence the lower the anticipated heat transfer rate. This had the advantage of limiting the gross power required, but also carried the disadvantage of reduced accuracy in calculating the net heat transfer rate. Comparatively low heat transfer rates are to be expected with air, for which the product $\nu\kappa$ is several orders of magnitude greater than for typical non-metallic liquids. This was partly offset in the experiments by using a wider range of $(T_w - T_a)$ than would likely occur in the field, but the range of t_d studied still represents the lower end of the anticipated field range. The experiments therefore provided a strenuous practical test of the wind augmentation idea and generated conservative heat transfer data. Table 1 lists the range of variables covered. For convenience, the wind and its internal component are shown in both dimensional and non-dimensional form.

Table 1. Test schedule ($L/D = 10:1$, $3 < \log_{10} t_D < 4$)

Test	L_i/L	U_∞(m s^{-1})	ΔP(Pa)	$\bar{U}$(m s^{-1})	Re
1	0.50	0	0	0	0
2	0.50	5	8.7	2.0	500
3	0.50	10	32	6.0	1430
4	0.50	20	80	11	2550
5	0.75	0	0	0	0
6	0.75	5	8.5	1.9	460
7	0.75	10	36	5.2	1250
8	0.75	20	87	10	2390
9	0.90	0	0	0	0
10	0.90	5	4.5	0.92	230
11	0.90	10	40	5.5	1320
12	0.90	20	95	10	2460

DISCUSSION OF RESULTS

General remarks

It is clear that the effect of wind augmentation on the performance of an open thermosyphon tube must be treated as a problem of combined free and forced convection. Unfortunately, there is no published regime map for a concentric tube system in which the inner tube length is a variable. The nearest map equivalent appears to be that produced by Metais and Eckert [13] for a single vertical tube. Table 1 reveals that $10^3 < t_D < 10^4$ and $0 < Re < 2550$, for which ranges the Metais and Eckert map indicates the existence of several regimes: laminar free convection, laminar forced convection, mixed laminar convection and forced turbulent convection. It is fairly certain that inter-regime transitions—the laminar–turbulent transition in particular—will further complicate the flow description.

The open tube thermosyphon exhibits other regime behaviour, as may be seen from Fig. 4 which presents the experimental results of Martin, for air, along with the theoretical predictions of Lighthill, for a Prandtl number of 1.0. The theoretical curves clearly distinguish between the higher heat transfer rates of the boundary layer regime and the lower values characteristic of the impeded regime. As mentioned earlier, only large diameter thermosyphon tubes would be capable of producing a boundary layer flow in practice.

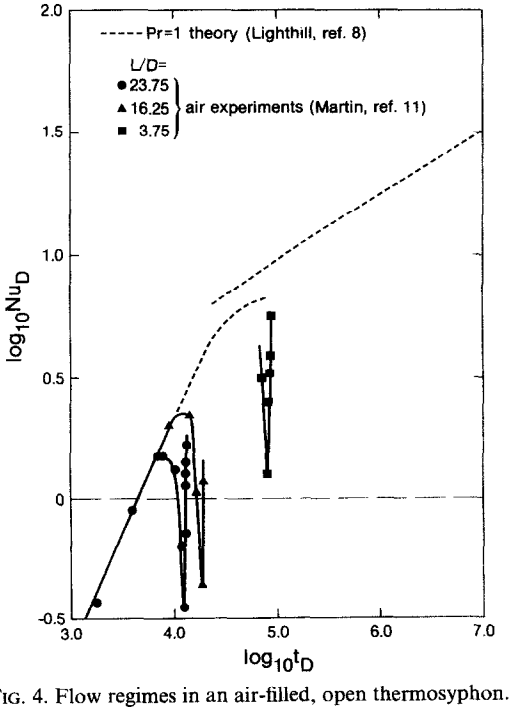

FIG. 4. Flow regimes in an air-filled, open thermosyphon.

At first sight, the experimental data appear to be anomalous, or badly scattered, but in fact they are not. They reveal that as t_D is increased from a value well down in the impeded regime, the heat transfer rate first follows the theoretical curve but eventually experiences a maximum followed by a very sharp decline which, in turn, is followed by an equally sharp rise. It is speculated that if t_D were increased sufficiently the experimental results would eventually rejoin the theoretical curve in the boundary layer regime.

The cause of this dramatic chasm is uncertain but is believed to be associated with flow conditions in general, and stability in particular, near the mouth of the thermosyphon. As t_D decreases below about 10^6, the interaction between the exiting boundary layer and the entering core increases. The exiting flow is known to interfere with the surrounding fluid well removed from the tube mouth [9]. Only further experimentation, preferably with flow visualization, would clarify the behaviour.

It is tempting to assume that the inherent instability of the exiting annular 'jet' is the cause of the behaviour but this cannot provide a full explanation because the same chasm has been observed in a closed tube thermosyphon filled with air [14]. It is certain, however, that the behaviour does not simply reflect a transition from laminar to turbulent flow which usually requires t_D values several orders of magnitude greater. For the present purposes, it is sufficient to note that increasing mutual interference resulting from a decreasing t_D in the boundary layer regime eventually creates a choking-stagnation effect which is maintained over a small range until a lower value of t_D establishes a stable, impeded flow. The importance of these observations will be apparent later.

The accuracy of the experimental data presented below was established by an error analysis which revealed, in general terms, that the uncertainty in the Nusselt number decreased as the wind speed increased. Error bars are shown on various curves in Figs. 5 and 7, from which it is apparent that difficulties in measuring heat fluxes of the order of a few watts restrict the use of the low wind and no-wind data to a qualitative role.

Effect of insert tube

The effect of varying the insert tube length is shown in Fig. 5 for each of three wind speeds, represented in convenient dimensional form. The curves shown are hand drawn and are faired through individual data sets merely to assist the eye. At high wind speeds it is evident that increasing the length of the insert tube leads to an increase in heat transfer rate, whereas at lower speeds (the no-wind data are not shown) the trend is reversed. The explanation of this reversal may be found in the relative importance of two adverse factors: the viscous drag exerted by the insert and the creation of a relatively stagnant pool of air at the bottom of the thermosyphon. When the wind plays

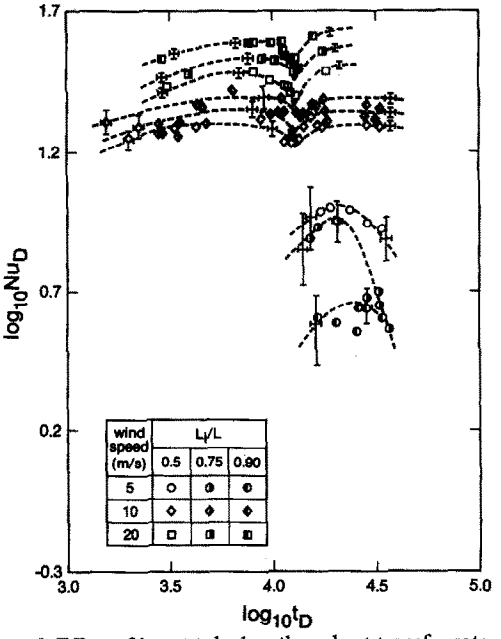

FIG. 5. Effect of insert tube length on heat transfer rate.

only a small role, the effect of lengthening the insert is to further reduce velocities which are not too different from the low values associated with the impeded regime: lengthening the insert thereby reduces the heat transfer rate.

On the other hand, when the wind plays an important part in circulating the air, the bottom end of the insert tube marks the top of a region in which the flow turns through 180°. Beneath this 'turning region', the air flow will be governed largely by the much weaker buoyancy forces. Under such conditions, decreasing the insert length merely moves the 'turning region' further up the thermosyphon tube creating beneath a larger pool of air in which heat transfer rates are essentially those of an impeded regime.

This explanation is supported by the data plotted in Fig. 6 using the $t_D = 10^{4.0}$ data (or extrapolation) of each curve in Fig. 5 in addition to a single no-wind point. Broken lines are extrapolations. Although limited, these data suggest that an insert length of about one half the thermosyphon tube length would be an optimal choice. The extent of the 'turning region' is unknown but the data suggest it is at least one diameter long. In fact, it may not be sharply defined and may gradually merge with the impeded flow beneath.

The experimental results reported here were obtained with the ratio d/D close to 0.7071, as noted earlier. This is a convenient choice which avoids excessive flow resistance caused by either of the inner or outer flow areas being overly constricted. However, d/D is an important design parameter and deserves further attention.

Effect of wind speed

It is clear from Fig. 5 that the chasm of the pure air-filled thermosyphon has re-appeared in the mixed

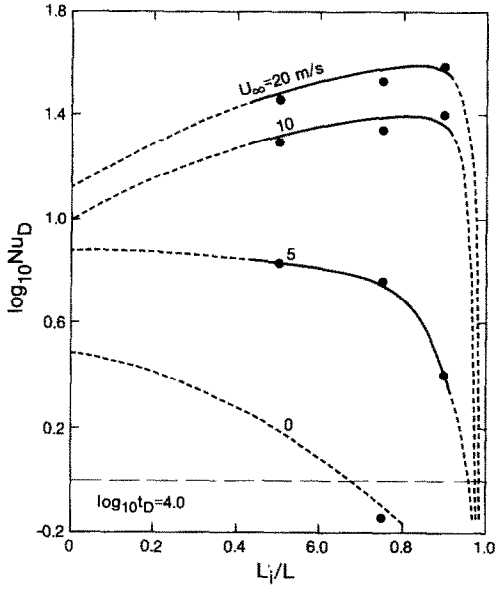

FIG. 6. Optimizing insert tube length.

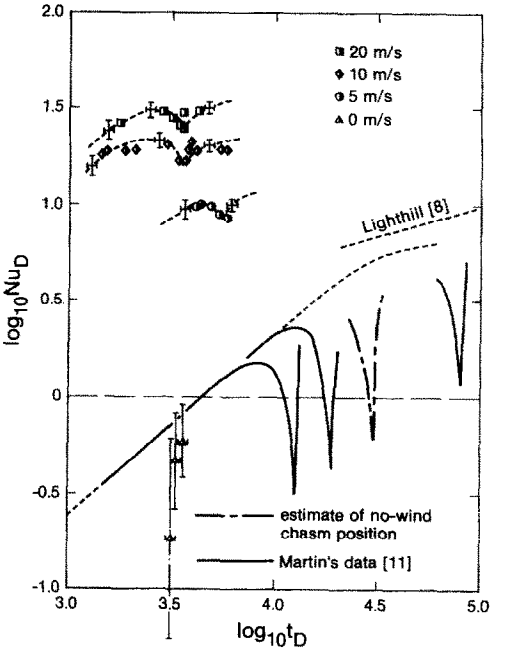

FIG. 7. Effect of wind speed: $L_i/L = 0.50$.

flow situation. This seems to throw doubt on the inlet choking-stagnation hypothesis of performance deterioration because the insert tube prevents any mixing in the inlet region. However, the bottom end of the insert creates a false mouth within the thermosyphon and it is quite likely that pseudo-entry behaviour occurs in the vicinity of it. Although this is a local effect, which would be limited only to the air beneath, it should still appear in the overall heat transfer curves.

Figures 5 and 7 generally confirm this expectation and reveal that the effect decreases as the wind speed increases. It is also evident that wind speed influences the location of the chasm. Given the choking-stagnation hypothesis, it is to be expected that the effect of the wind would be to further destabilize the flow and thus shift the t_D range over which it would occur. Although this is a reasonable expectation, the complexity of stability in an opposed free–forced convection flow demands that the hypothesis be treated as a speculation. Even so, the data of Fig. 7 (and other data not shown) support it and suggest that the destabilizing effect is most marked when the wind speed increases from zero to magnitudes of the order of 5 m s^{-1}; further increases in wind speed have a diminishing effect, but the overall reduction in t_D at the base of the chasm is seen to be about an order of magnitude as wind speed increases from 0 to 20 m s^{-1}.

From a heat transfer standpoint, perhaps the most significant feature of Fig. 7, which includes no-wind data, is the performance improvement introduced by the wind. It is not likely that a wind speed of 20 m s^{-1} would be maintained over a long period of time in practice but more realistic average values in the range 5–10 m s^{-1} are seen to be capable of producing substantial increases in the heat transfer rate above the no-wind values. Improvements of about an order of magnitude reveal that the performance of the system is then comparable with the lower range of the boundary layer regime, thus bringing heat transfer rates up into a practical range, at least for geotechnical applications. In fact, these values are conservative because much larger tube diameters would be used in practice where the monotonically increasing trend suggested in Fig. 7 (to the right of the chasms) implies field heat transfer rates which may well be an order of magnitude greater than those shown. Only experiments with large-diameter, air-filled tubes could confirm this.

Empirical correlation

As noted earlier, the regime map of Metais and Eckert suggests that the data reported here may cover distinct regimes along with the corresponding inter-regime transitions. This range of possibilities is supported by the range of parameters Ra, Re and Ra/Re^2. At first glance, the development of a correlation to cover all these prospects would seem to be a daunting task. None the less, an attempt was made using the mixed empirical form

$$Nu_D = a\left(\frac{L_i}{L}\right)[Gz + bt_i^m]^n \tag{1}$$

in which the Graetz number was defined by

$$Gz = \frac{\bar{U}(D-d)^2}{\kappa L_i}$$

and $t_i = Ra_D D/(L-L_i)$. These were chosen in order to

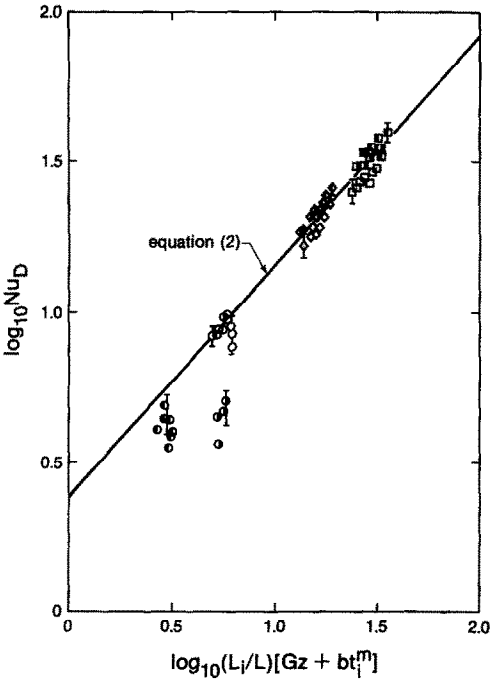

FIG. 8. Empirical heat transfer correlation.

incorporate both mixed convection in the annulus,† considered to be the major effect, and free convection beneath the insert tube, considered to be a minor effect. It was hoped that changes in the flow regime would be incorporated through m and n.

By trial and error, it was found that with $m = 1/n$, the data could be related by the equation

$$Nu_D = 2.36\frac{L_i}{L}[Gz + 8 \times 10^{-7} t_i^{1.3}]^{0.77} \qquad (2)$$

which is shown plotted with the experimental data in Fig. 8. Within the limits of experimental error, it is evident that equation (2) adequately correlates the data, but the result requires further discussion. To begin with, the apparent scatter would be expected to be greater than the restricted form of equation (1) might suggest because of changes from regime to regime. This is particularly true of the chasm behaviour which is clearly not monotonic, thus giving rise to some doubt in the choice of m. The relation $m = 1/n$ was chosen to preserve the known behaviour of an open thermosyphon in the impeded regime ($mn = 1$), but the comparatively small effect of free convection shown does not provide an adequate test of the assumption. By the same token, some of the data in the low end of the range are too scattered to test the correlation, but since they contain well-defined chasms it is not surprising to find that they are anomalous.

† For which a Rayleigh number based on $D-d$ would be more appropriate but would present a conflict with the empty tube definition necessary for comparative purposes.

To a first approximation, equation (2) suggests that forced convection was dominant for Nusselt numbers in excess of 10 (abscissa values greater than $10^{0.75}$). The value of n suggests a turbulent flow but the range of Reynolds numbers listed in Table 1 (and the range of Ra/Re^2) indicates that this would only be likely at the very highest wind speed, unless the 'turning region' created turbulent mixing at lower Reynolds numbers. In any event, equation (2) would probably apply above the range tested, thus suggesting a heat transfer performance well into the range normally associated with boundary layer flow. On the other hand, extrapolation below the test range is not recommended until the precise effect of the chasms is better known.

CONCLUSIONS

The principal conclusion to be reached from the above results is the substantial increase in heat transfer rate which can be produced by the wind. At relatively high average wind speeds (10–20 m s^{-1}) the improvement raises the heat transfer rate up to values normally associated with the more efficient boundary layer regime. In a geotechnical context, such increases suggest that the use of on-site air compressors to provide forced flow during crucial construction periods may be a useful alternative : e.g. during the initial freezing period or when wind speed and/or the prevailing temperature difference is too low. However, even when the average wind speed is in the more practical range of 5–10 m s^{-1}, it is clear that the heat transfer rates benefit significantly from the superimposed forced convection effect.

In such a mixed convection system the role of the insert tube is very important. In general terms, it increases viscous drag on the one hand while reducing convective impedance on the other. The relative importance of these two effects varies with wind speed, the drag effect being more important when the wind speed is low. At higher wind speeds, the dominance of the thermal impedance control mechanism was clearly evident in the increase in heat transfer rate produced by increasing the insert tube length. For the range of conditions considered, the optimum length of the insert tube appeared to be about half the length of the thermosyphon tube.

The characteristic 'chasm' seen in previous thermosyphon data was also observed in data recorded here. Given that its cause is rooted in instability near the mouth of the thermosyphon, it should re-appear at the false mouth created immediately beneath the lower end of the insert tube. This expectation was confirmed, with the effect being gradually reduced as the wind speed increased.

Treating the problem as a special case of mixed convection, an attempt was made to correlate the data in conventional form. Within an accuracy of $\pm 6\%$ the correlation was successful for Nusselt numbers greater than about 10 : that is for $(Gz + 8 \times 10^{-7} t_i^{1.3})L_i/L$ greater than about $10^{0.75}$.

Acknowledgements—This work was undertaken with the support of the Natural Sciences and Engineering Research Council of Canada to whom the authors are grateful. We would also like to thank Mr T. Nord, Mr T. Villett, Mr A. Muir and the workshop staff of the Department of Mechanical Engineering, University of Alberta.

REFERENCES

1. F. J. Bayley, Heat transfer characteristics of the closed thermosyphon, Ph.D. thesis, University of Durham (1955).
2. E. Schmidt, Heat transmission by natural convection at high centrifugal acceleration in water-cooled gas turbine blades, *Proc. Instn Mech. Engrs* 361 (1951).
3. D. Japiske, Heat transfer in open and closed thermosyphons, Ph.D. thesis, Purdue University (1968).
4. G. F. Biyanov, V. I. Makarov and A. D. Molochnikov, Liquid cooling unit for freezing thawed ground and cooling plastically frozen ground for construction in areas with harsh climates, *Proc. Second Int. Permafrost Conf., N.A.S.*, pp. 641–643 (1973).
5. H. O. Jahns, T. W. Miller, L. D. Power, V. P. Ricki, T. P. Taylor and J. A. Wheeler, Permafrost protection for pipelines, *Proc. Second Int. Permafrost Conf., N.A.S.* (1973).
6. Peace-Athabasca Delta Project Report, Intergovernmental Study Group, Dept. Environment Queen's Printer (1972).
7. G. S. H. Lock, The BIVA project, *Proc. IAHR Ice Symposium*, Vol. II, pp. 269–280 (1986).
8. M. J. Lighthill, Theoretical considerations on free convection in tubes, *Q. J. Mech. Appl. Math.* **6**(4), 398–439 (1953).
9. D. Japiske and E. R. F. Winter, Single-phase transport processes in the open thermosyphon, *Int. J. Heat Mass Transfer* **14**, 427–441 (1971).
10. F. M. Leslie and B. W. Martin, Laminar flow in the open thermosyphon with special reference to small Prandtl numbers, *J. Mech. Engng Sci.* **1**(2), 184–193 (1959).
11. B. W. Martin, Free convection in an open thermosyphon with special reference to turbulent flow, *Proc. R. Soc.* **A230**, 502–530 (1955).
12. R. L. Reid, J. S. Tennant and K. W. Childs, The modelling of a thermosyphon type permafrost protection device, *J. Heat Transfer* **97**(2), 382–386 (1975).
13. B. Metais and E. R. G. Eckert, Forced, mixed and free convection régimes, *J. Heat Transfer* **86**, 295 (1964).
14. F. J. Bayley and G. S. H. Lock, Heat transfer characteristics of the closed thermosyphon, *J. Heat Transfer* **87**, 30–40 (1965).

PERFORMANCE D'UN TUBE THERMOSIPHON OUVERT A AIR, AVEC REFERENCE PARTICULIERE A L'AUGMENTATION DE VENT

Résumé—On étudie expérimentalement le thermosiphon ouvert à air. A la suite d'une revue des régimes des thermosiphons, avec une attention particulière portée au cas de l'air, on décrit une série d'expériences. Elle est conduite pour explorer l'effet d'un écoulement forcé superposé et dû à des courants d'air. Cet effet et l'arrangement tubulaire qui est nécessaire sont discutés d'un point de vue thermique.

VERHALTEN EINES LUFTGEFÜLLTEN OFFENEN THERMOSYPHONS UNTER BESONDERER BERÜCKSICHTIGUNG VON WINDEINFLÜSSEN

Zusammenfassung—Diese Arbeit behandelt die experimentelle Untersuchung eines luftgefüllten offenen Thermosyphons. Nach einer Übersicht zu Thermosyphonsystemen—unter besonderer Berücksichtigung des unüblichen Verhaltens von Luft—wird eine Reihe von Experimenten beschrieben. Diese wurden durchgeführt, um den Einfluß einer überlagerten erzwungenen Strömung zu untersuchen, die von auftretenden Winden erzeugt wird. Der Windeffekt und die Rohranordnung, die zu seiner Kanalisierung führt, werden dann vom Standpunkt der Wärmeübertragung aus diskutiert.

РАЪОЧИЕ ХАРАКТЕРИСТИКИ ОТКРЫТОГО ТЕРМОСИФОНА, ЭАПОЛНЕННОГО ВОЗДУХОМ, С УЧЕТОМ УСИЛЕНИЯ ВОЗДУШНОЙ СТРУИ

Аннотация—Представлено экспериментальное исследование заполненного воздухом открытого термосифона. Рассмотрены режимы работы термосифона, причем особое внимание уделено нетипичным свойствам, связанным с воздухом. Описана серия экспериментов, проведенных в этих режимах. Указанные экспериименты провоедены с целью изучения влияния наложенного вынужденного потока, вызванного преобладающими струями воздуха. Обсуждаются эффекты струи воздуха и необходимое для его передачи расположение трубн с точки зрения теплопереноса.